

## Speed of rolling droplets

Ehud Yariv

*Department of Mathematics, Technion—Israel Institute of Technology, Haifa 32000, Israel*

Ory Schnitzer

*Department of Mathematics, Imperial College London, London SW7 2AZ, United Kingdom*



(Received 2 May 2019; published 3 September 2019)

We analyze the near-rolling motion of two-dimensional nonwetting drops down a gently inclined plane. Inspired by the scaling analysis of Mahadevan and Pomeau [*Phys. Fluids* **11**, 2449 (1999)], we focus upon the limit of small Bond numbers,  $B \ll 1$ , where the drop shape is nearly circular and the internal flow is approximately a rigid-body rotation except close to the flat spot at the base of the drop. Our analysis reveals that the leading-order dissipation is contributed by both the flow in the flat-spot region and the correction to rigid-body rotation in the remaining liquid domain. The resulting leading-order approximation for the drop velocity  $\mathcal{U}$  is given by  $\mu\mathcal{U}/\gamma \sim \alpha/2B \ln \frac{1}{B}$ , wherein  $\mu$  is the liquid viscosity,  $\gamma$  the interfacial tension, and  $\alpha$  the inclination angle.

DOI: [10.1103/PhysRevFluids.4.093602](https://doi.org/10.1103/PhysRevFluids.4.093602)

### I. INTRODUCTION

The motion of a liquid drop down a gently tilted nonwetted solid in some cases resembles rigid-body rolling. For a drop to roll, it must be sufficiently small and the contact angle sufficiently large such that its shape remains nearly spherical; at the same time, contact-angle hysteresis must be sufficiently weak so that the drop does not stick to the solid. Mahadevan and Pomeau [1] identified the scaling law for steady rolling of a drop showing, counterintuitively, that its speed is inversely proportional to its size. Using superhydrophobic surfaces [2], this surprising prediction has been confirmed experimentally [3–5].

The scaling analysis of Mahadevan and Pomeau [1] exploits the necessary smallness of the drop relative to the capillary length (small Bond number  $B$ ). In that limit, and for a small inclination angle  $\alpha$ , the drop shape remains nearly spherical, with only a small “flat spot” in contact with the solid; the flow is accordingly a rigid-body rotation except in a small region close to the flat spot. By estimating the viscous dissipation in the latter region and comparing it to the time rate of change of gravitational potential energy, Mahadevan and Pomeau found the drop velocity (normalized by interfacial tension over viscosity) to scale as  $\alpha/B^{1/2}$ . The above scaling analysis assumes an idealized nonwetting solid, where the contact angle is precisely  $180^\circ$ . In that case, the singularity usually arising at a moving contact line [6] is alleviated [7]. To demonstrate this, Mahadevan and Pomeau [1] supplemented their scaling arguments with a local two-dimensional corner analysis close to the contact line (on scales small compared with the flat spot), based on the rationale that two- and three-dimensional flows share similar features.

The rolling-drop problem presents a rare example of a well-posed moving-contact-line problem. Nonetheless, we are not aware of any analytical studies attempting to calculate the rolling speed or describe the liquid flow field. Perhaps the most relevant analytical study is that of Hodges *et al.* [8], who considered a set of closely related problems involving both two- and three-dimensional liquid drops surrounded by another fluid and moving parallel to a solid substrate. As pointed out by Hodges *et al.* [8], their models reduce in certain limits to the rolling regime described in Ref. [1].

Unfortunately, only scaling results were provided in those specific limits; it was argued by Hodges *et al.* that, even in two dimensions, a detailed analysis would necessarily entail boundary-integral calculations over the whole interior of the drop. For later reference, we note that Hodges *et al.* [8] give  $\alpha/B$  as the two-dimensional equivalent of the Mahadevan-Pomeau velocity scaling.

Our goal is an asymptotic analysis of drops rolling down a gently inclined nonwetting surface. Due to the complexity of the problem, we elect to start here by considering two-dimensional drops; this choice is further motivated by the local solution of Mahadevan and Pomeau [1] and the availability of numerical simulations in two dimensions [9–11]. To this end, we shall adopt an approach similar to that of Hodges *et al.* [8], where the flow problem to be solved is obtained by linearization about the reference static shape of the drop. Both the static shape and the resulting linearized flow are characterized by a single parameter, the Bond number. We analyze the small-Bond-number limit pertinent to rolling droplets analytically. To that end, we utilize the method of matched asymptotic expansions [12], separately analyzing the flat-spot region and drop-scale region.

## II. FORMULATION

A two-dimensional liquid drop (density  $\rho$ , viscosity  $\mu$ ) of area  $\pi a^2$  is placed upon a solid plane which is inclined at an angle  $\alpha$  relative to the horizontal. The contact angle is  $180^\circ$ . Our interest lies in the drop velocity down the plane, say,  $\mathcal{U}$ : it is defined as the velocity of a reference system in which the flow problem is steady.

We employ a dimensionless formulation, normalizing length variables by  $a$ , stress variables by  $\gamma/a$ , and velocity variables by  $\gamma/\mu$ . The dimensionless drop velocity  $\mu\mathcal{U}/\gamma$  is denoted by  $\omega$ . If the drop were rotating as a rigid circle,  $\omega$  would represent its angular velocity (normalized by  $\gamma/\mu a$ ). We attach the Cartesian coordinates  $(x, y)$  to the comoving reference frame, with the  $x$  axis lying on the plane while the  $y$  axis passes through the drop centroid. We additionally employ the  $(r, \theta)$  coordinates, defined by

$$x = r \cos \theta, \quad y = r \sin \theta. \quad (2.1)$$

The body force (normalized by  $\gamma/a^2$ ) experienced by the liquid is

$$B(\hat{\mathbf{e}}_x \sin \alpha - \hat{\mathbf{e}}_y \cos \alpha) \quad (2.2)$$

in which  $B = \rho g a^2 / \gamma$  is the Bond number.

Dimensional analysis implies that  $\omega$  is a function of  $\alpha$  and  $B$ . For gentle slopes,  $\alpha \ll 1$ , where  $\omega$  is proportional to  $\alpha$ :

$$\omega/\alpha = \text{a function of } B. \quad (2.3)$$

Our goal is to evaluate that function in the limit  $B \ll 1$ .

## III. STATIONARY SHAPE

We begin with calculating the stationary shape at  $\alpha = 0$ ; see Fig. 1. It is symmetric about the  $y$  axis, with a flat spot between two detachment points at  $(\pm l, 0)$ , wherein  $l$  is a constant to be determined. Following Rienstra [13] we employ the intrinsic inclination angle  $\phi$ , in terms of which  $\hat{\mathbf{n}} = \hat{\mathbf{e}}_x \sin \phi - \hat{\mathbf{e}}_y \cos \phi$  is the unit normal pointing outward and  $\hat{\mathbf{t}} = \hat{\mathbf{e}}_x \cos \phi + \hat{\mathbf{e}}_y \sin \phi$  is a unit tangent. The curvature is  $d\phi/ds$ , where  $s$  is the arc length measured from the detachment point  $(l, 0)$ .

The distribution of the pressure  $p$  is clearly hydrostatic, say,  $p^* - By$ , wherein the flat-spot pressure  $p^*$  remains to be determined. The Young-Laplace law reads

$$\frac{d\phi}{ds} = p^* - By. \quad (3.1)$$

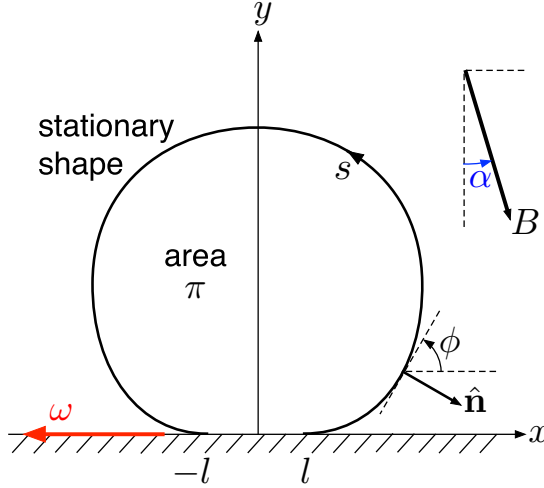


FIG. 1. The stationary shape is attained at  $\alpha = 0$ . For  $0 < \alpha \ll 1$  the flow problem is solved about that reference shape.

The dependence of  $\phi$  upon  $s$  is determined by this equation, together with the “initial” condition

$$\phi(0) = 0, \quad (3.2)$$

representing the presumed  $180^\circ$  Young angle. When regarded as functions of  $s$ ,  $x$  and  $y$  are governed by the equations

$$\frac{dx}{ds} = \cos \phi, \quad \frac{dy}{ds} = \sin \phi \quad (3.3)$$

and the “initial” conditions

$$x(0) = l, \quad y(0) = 0. \quad (3.4)$$

With no loss of generality we restrict the calculation to  $x > 0$ , where  $0 < \phi < \pi$ . It is then convenient to employ  $\phi$  as the independent variable, instead of  $s$ . Substituting (3.1) into (3.3) then gives

$$\frac{dx}{d\phi} = \frac{\cos \phi}{p^* - By}, \quad \frac{dy}{d\phi} = \frac{\sin \phi}{p^* - By}, \quad (3.5)$$

where  $x$  and  $y$  are now understood to be functions of  $\phi$ . With that slight abuse of notation, the initial conditions (3.4) remain valid.

Integration of (3.4) and (3.5) provides the shape in terms of the parameters  $p^*$  and  $l$ . The constant  $p^*$  is determined from the area-conservation constraint,

$$\int_0^\pi x \frac{dy}{d\phi} d\phi = \frac{\pi}{2}, \quad (3.6)$$

while the detachment location  $l$  is determined from the integral force balance,

$$p^* l = \frac{\pi}{2} B. \quad (3.7)$$

In principle, the above procedure may be employed to evaluate the drop shape for arbitrary values of  $B$ . We focus here upon the limit  $B \ll 1$ . The force balance (3.7) implies  $l = O(B)$ , whereby we

readily find from (3.4)–(3.6) the leading-order approximations

$$x = \sin \phi + \dots, \quad (3.8a)$$

$$y = 1 - \cos \phi + \dots \quad (3.8b)$$

and

$$p^* = 1 + \dots, \quad (3.9)$$

with  $O(B)$  corrections. This leading-order approximation simply corresponds to a circular drop. Substitution of (3.9) into (3.7) yields the leading-order approximation for the size of the flat spot:

$$l = B \frac{\pi}{2} + \dots. \quad (3.10)$$

The above expansions for  $x$  and  $y$  are understood to describe the drop scale. It is clear from (3.8a) that  $x$  becomes comparable to  $l$  for  $\phi = O(B)$ . To describe the stationary shape of the drop in that flat-spot region, we write  $\phi = B\Phi$  and define the stretched coordinates

$$X = x/B, \quad Y = y/B. \quad (3.11)$$

Regarding  $X$  and  $Y$  as functions of  $\Phi$ , we find from (3.5) and (3.9)

$$\frac{dX}{d\Phi} = 1 + \dots, \quad \frac{dY}{d\Phi} = B\Phi + \dots, \quad (3.12)$$

together with the initial conditions  $X(0) = \pi/2 + \dots$  and  $Y(0) = 0$  [cf. (3.4) and (3.10)]. Thus to leading order we have the locally parabolic profile

$$X = (\pi/2 + \Phi) + \dots, \quad Y = B \frac{\Phi^2}{2} + \dots. \quad (3.13)$$

#### IV. FLOW

We now allow for a gentle slope,  $\alpha \ll 1$ . We employ the following linearization:

$$\mathbf{u} = \alpha \tilde{\mathbf{u}}, \quad p = p^* - By + \alpha \tilde{p}, \quad (4.1)$$

where  $\tilde{\mathbf{u}} = \hat{\mathbf{e}}_x \tilde{u} + \hat{\mathbf{e}}_y \tilde{v}$ , with the associated linearizations of the drop velocity and rate-of-strain tensor

$$\boldsymbol{\omega} = \alpha \tilde{\boldsymbol{\omega}}, \quad \mathbf{e} = \alpha \tilde{\mathbf{e}}. \quad (4.2)$$

At leading order in  $\alpha$  the resulting flow is associated with the stationary shape. It is governed by the continuity and inhomogeneous Stokes equations [cf. (2.2)],

$$\nabla \cdot \tilde{\mathbf{u}} = 0, \quad \nabla \tilde{p} = \nabla^2 \tilde{\mathbf{u}} + B \hat{\mathbf{e}}_x. \quad (4.3)$$

At  $y = 0$  it satisfies no-slip and impermeability,

$$\tilde{\mathbf{u}} = -\tilde{\omega} \hat{\mathbf{e}}_x. \quad (4.4)$$

At the free surface it satisfies the dynamic shear-free condition,

$$\hat{\mathbf{n}} \hat{\mathbf{t}} : \tilde{\mathbf{e}} = 0, \quad (4.5)$$

as well as kinematic impermeability,

$$\hat{\mathbf{n}} \cdot \tilde{\mathbf{u}} = 0. \quad (4.6)$$

For a given value of  $B$ , the preceding problem provides the linearized flow in terms of the drop velocity  $\tilde{\omega}$ . The latter is determined by the energy balance,

$$2 \iint \tilde{\mathbf{e}} : \tilde{\mathbf{e}} \, dx \, dy = \pi B \tilde{\omega}, \quad (4.7)$$

where the left-hand side, in which the integration is carried out over the reference drop domain, represents the integral dissipation rate (per unit length), while the right-hand side represents the rate of loss of gravitational potential energy (per unit length). Since the dissipation is unaffected by a Galilean transformation, we may employ the rate-of-strain tensor in the comoving frame.

Three observations are warranted. First, since the flow problem (4.3)–(4.6) is linear and homogeneous in  $\tilde{\omega}$ , the left-hand side of (4.7) is proportional to  $\tilde{\omega}^2$ . Second, the symmetry of the reference shape about the  $y$  axis implies that  $\tilde{u}$  is an even function of  $x$  while  $\tilde{v}$  is an odd function of it. The third observation is that the dynamic pressure  $\tilde{p}$  is determined by (4.3)–(4.6) only up to an additive constant. The unique determination of the pressure requires the use of the normal-stress boundary condition [see (3.1)] at  $O(\alpha)$ ; at that order, however, the condition is affected by the  $O(\alpha)$  deviations from the reference shape, whose calculation we wish to avoid. Fortunately, the dynamic pressure distribution is not required in the subsequent analysis.

## V. SMALL DROP

For  $B \ll 1$  the drop is approximately circular. In most of the drop domain the flow is given by a superposition of the uniform velocity (4.4) and rigid-body rotation. Such a rigid-body motion, however, is kinematically incompatible with the flat spot about the origin. In what follows we employ the method of matched asymptotic expansions [12], separately analyzing the flat-spot region, of  $O(B)$  extent, and the drop-scale region, where the flat spot appears as a point singularity.

We begin by determining the scaling, say,  $\chi(B)$ , of the velocity gradients within the flat-spot region. Because of asymptotic matching, that is also the scaling of the velocity gradients in the drop-scale region, and whence the scaling of the velocity itself. It follows that the right-hand side of (4.7) is  $O(B\chi)$ . The contribution of the flat-spot region to the left-hand side of (4.7) is clearly  $O(B^2\chi^2)$ . Since that contribution is expected to appear at leading order [1], we conclude that  $\chi = 1/B$ . It is then convenient to define the leading-order drop velocity,

$$\tilde{\omega} = B^{-1}\Omega + \dots \quad (5.1)$$

Consider now the drop-scale region. At leading order, the flow there is provided by a rigid-body motion which is consistent with (5.1):

$$\tilde{\mathbf{u}} = B^{-1}\Omega[(y-1)\hat{\mathbf{e}}_x - x\hat{\mathbf{e}}_y] + \dots \quad (5.2)$$

This solution trivially satisfies Eqs. (4.3) and conditions (4.5) and (4.6).

The flat-spot region is described in terms of the stretched coordinates (3.11) as well as the corresponding polar coordinates  $(R, \theta)$ , defined by [cf. (2.1)]

$$X = R \cos \theta, \quad Y = R \sin \theta. \quad (5.3)$$

In view of (3.10), the detachment points in the  $XY$  plane are  $(\pm\pi/2, 0)$ . To obtain the shape of the free boundary close to these points we invert (3.13) to obtain

$$Y = B \frac{(X \mp \pi/2)^2}{2} + \dots \quad \text{for } X \gtrless \pi/2. \quad (5.4)$$

At leading order, then, the flat-spot region is provided by the upper-half of the  $XY$  plane; see Fig. 2.

The  $O(B^{-1})$  velocity gradients imply  $O(1)$  velocities in the flat-spot region; condition (4.4) thus implies a combination of an  $O(B^{-1})$  uniform velocity with an  $O(1)$  spatially varying field. We accordingly write

$$\tilde{\mathbf{u}} = -\tilde{\omega}\hat{\mathbf{e}}_x + \mathbf{U}, \quad \tilde{p} = B^{-1}P, \quad (5.5)$$

where the flat-spot fields  $\mathbf{U} = \hat{\mathbf{e}}_x U + \hat{\mathbf{e}}_y V$  and  $P$  are  $O(1)$  functions of  $X$  and  $Y$ . Note that (i)  $\mathbf{U}$  constitutes the fluid velocity in the laboratory reference frame and (ii)  $\tilde{\omega}$  may also possess an  $O(1)$  term. As that term does not play a role in the subsequent analysis we have omitted it in Eq. (5.1).

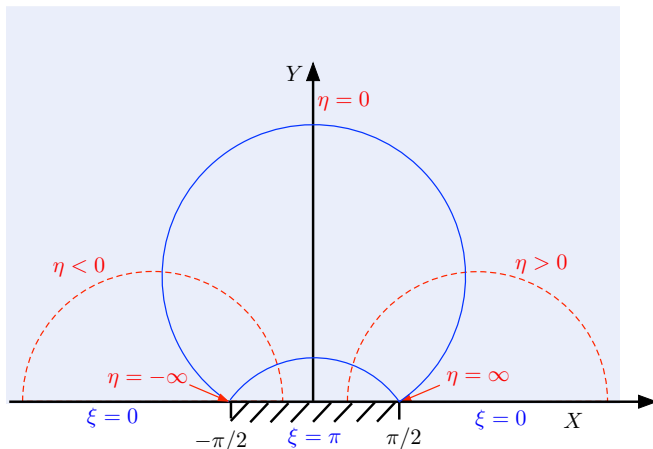


FIG. 2. The upper-half  $XY$  plane. Also shown are constant- $\xi$  (solid) and constant- $\eta$  (dashed) arcs.

At leading order, the flat-spot flow is governed by the homogeneous Stokes equations [cf. (4.3)],

$$\frac{\partial U}{\partial X} + \frac{\partial V}{\partial Y} = 0, \quad \frac{\partial P}{\partial X} = \Delta U, \quad \frac{\partial P}{\partial Y} = \Delta V, \quad (5.6)$$

wherein  $\Delta = \partial^2/\partial X^2 + \partial^2/\partial Y^2$ . At  $Y = 0$  it satisfies the impermeability and no-slip conditions for  $|X| < \pi/2$  [cf. (4.4)],

$$V = 0, \quad U = 0, \quad (5.7)$$

and a shear-free condition for  $|X| > \pi/2$  [cf. (4.5)],

$$\frac{\partial U}{\partial Y} + \frac{\partial V}{\partial X} = 0. \quad (5.8)$$

At large  $R$ , it satisfies asymptotic matching with the rigid-body motion (5.2), whereby

$$U \sim \Omega Y, \quad V \sim -\Omega X \quad \text{for } R \gg 1. \quad (5.9)$$

Last, we need to impose the free-surface kinematic condition (4.6) at  $Y = 0$ . This requires some care, as the large velocity (5.1) necessitates to account for the small parabolic correction (5.4). This gives the *inhomogeneous* condition

$$\Omega(X \mp \pi/2) + V = 0 \quad \text{for } X \gtrless \pi/2, \quad (5.10)$$

which is consistent with (5.9). [Since the shear-free condition (4.5) is independent of the  $O(B^{-1})$  drop velocity, correction (5.4) does not affect (5.8).]

With (5.9) and (5.10) providing the only inhomogeneous conditions, it is evident that  $\mathbf{U}$  is linear and homogenous in  $\Omega$ , which is the quantity of interest.

## VI. STREAMFUNCTION FORMULATION

It is convenient to employ the streamfunction  $\Psi$ ,

$$U = \Omega \left( Y + \frac{\partial \Psi}{\partial Y} \right), \quad V = -\Omega \left( X + \frac{\partial \Psi}{\partial X} \right), \quad (6.1)$$

where we have factored out the dependence upon  $\Omega$  and subtracted off the rigid-body rotation (5.9). It is clear that  $\Psi$ , just like  $U$ , is an even function of  $X$ . Since it is defined to within an

arbitrary additive constant, we conveniently set it to zero at the detachment points  $(\pm\pi/2, 0)$ . The streamfunction is governed by (i) the biharmonic equation

$$\Delta^2\Psi = 0; \quad (6.2)$$

(ii) impermeability and no-slip at the solid surface [cf. (5.7)],

$$\Psi = \frac{(\pi/2)^2 - X^2}{2}, \quad \frac{\partial\Psi}{\partial Y} = 0 \quad \text{at } Y = 0 \quad \text{for } |X| < \pi/2; \quad (6.3)$$

(iii) impermeability and shear-free at the free surface [cf. (5.8) and (5.10)],

$$\Psi = \frac{\pi^2}{4} - \frac{\pi|X|}{2}, \quad \frac{\partial^2\Psi}{\partial Y^2} = 0 \quad \text{at } Y = 0 \quad \text{for } |X| > \pi/2; \quad (6.4)$$

and (iv) the requirement of  $o(R)$  velocities at large distances [cf. (5.9)],

$$\Psi = o(R^2) \quad \text{for } R \rightarrow \infty. \quad (6.5)$$

Note that  $\Psi$  represents the streamfunction of the excess flow, relative to the rigid-body rotation. The ‘‘total’’ streamfunction in the laboratory frame is defined as [cf. (6.1)]

$$U = \Omega \frac{\partial\Gamma}{\partial Y}, \quad V = -\Omega \frac{\partial\Gamma}{\partial X}. \quad (6.6)$$

With no loss of generality, we require that it, too, vanishes at the detachment points. We accordingly find that

$$\Gamma = \frac{X^2 + Y^2 - (\pi/2)^2}{2} + \Psi. \quad (6.7)$$

## VII. CALCULATION OF $\Psi$

The streamfunction  $\Psi$ , defined by the boundary-value problem (6.2)–(6.5), is conveniently calculated using bipolar coordinates (see Fig. 2), defined via the relations [14]

$$X = \frac{(\pi/2) \sinh \eta}{\cosh \eta - \cos \xi}, \quad Y = \frac{(\pi/2) \sin \xi}{\cosh \eta - \cos \xi}. \quad (7.1)$$

The constant- $\eta$  curves constitute a family of nonintersecting circles of radius  $(\pi/2)/|\sinh \eta|$ , centered about  $((\pi/2) \coth \eta, 0)$ . In the upper  $XY$  plane, the constant- $\xi$  curves constitute a family of circular arcs of radius  $(\pi/2)/\sin \xi$ , all passing through the limiting points  $(\pm\pi/2, 0)$ . In terms of these coordinates, the free surface is  $\xi = 0$ , the flat spot is  $\xi = \pi$ , and the fluid domain is the infinite strip  $-\infty < \eta < \infty, 0 < \xi < \pi$ . The infinity in the upper  $XY$  plane corresponds to  $\eta \rightarrow 0$  and  $\xi \rightarrow 0$ . In that limit

$$X \sim \frac{\pi\eta}{\eta^2 + \xi^2}, \quad Y \sim \frac{\pi\xi}{\eta^2 + \xi^2}, \quad (7.2)$$

whereby  $R^2 \sim \pi^2/(\eta^2 + \xi^2)$ .

In terms of the bipolar coordinates, the solid-surface conditions (6.3) become

$$\frac{\partial\Psi}{\partial\xi} = 0 \quad \text{at } \xi = \pi, \quad (7.3a)$$

$$\Psi = \frac{\pi^2}{8 \cosh^2(\eta/2)} \quad \text{at } \xi = \pi, \quad (7.3b)$$

while the free-surface conditions (6.4) read

$$\Psi = \frac{\pi^2}{4} \left( 1 - \frac{|\sinh \eta|}{\cosh \eta - 1} \right) \quad \text{at } \xi = 0, \quad (7.4a)$$

$$\frac{\partial}{\partial \xi} \left( \frac{1}{h^2} \frac{\partial \Psi}{\partial \xi} \right) - \frac{\partial}{\partial \eta} \left( \frac{1}{h^2} \frac{\partial \Psi}{\partial \eta} \right) = 0 \quad \text{at } \xi = 0, \quad (7.4b)$$

wherein

$$h = \frac{\pi/2}{\cosh \eta - \cos \xi} \quad (7.5)$$

is the metric coefficient of both  $\xi$  and  $\eta$ . The far-field condition (6.5) becomes

$$\Psi \ll (\xi^2 + \eta^2)^{-1} \quad \text{for } \xi, \eta \rightarrow 0, \quad (7.6)$$

and symmetry now implies that  $\Psi$  is an even function of  $\eta$ .

The standard practice [15] is to seek  $\Psi$  in the form

$$\frac{\int_0^\infty f(\xi, s) \cos \eta s \, ds}{\cosh \eta - \cos \xi}, \quad (7.7)$$

where the symmetry in  $\eta$  is trivially satisfied; the biharmonic equation implies that the kernel  $f$  is a superposition of the products

$$\cosh s\xi \cos \xi, \quad \cosh s\xi \sin \xi, \quad \sinh s\xi \cos \xi, \quad \sinh s\xi \sin \xi. \quad (7.8)$$

In the present problem, however, the cosine-transform structure (7.7) is incompatible with the inhomogeneous condition (7.4a). This is a nonconventional case where a singular eigenfunction must be introduced [16]. In particular, we attempt a solution where  $\Psi$  is a superposition of (7.7) and the following eigenfunction of the biharmonic equation (singular at  $\xi = \eta = 0$ ),

$$A \frac{\cos \xi}{\cosh \eta - \cos \xi}, \quad (7.9)$$

where the constant  $A$  remains to be determined. With that superposition, it is readily verified that satisfaction of the homogeneous conditions (7.3a) and (7.4b) necessitates the form [cf. (7.8)]

$$f(\xi, s) = C(s)[\cosh \xi s \cos \xi - s \sinh \xi s \sin \xi] + D(s)[\sinh \xi s \cos \xi - s \cosh \xi s \sin \xi]. \quad (7.10)$$

The inhomogeneous condition (7.4a) reads

$$\int_0^\infty C(s) \cos \eta s \, ds + A = \frac{\pi^2}{4} (e^{-|\eta|} - 1). \quad (7.11)$$

The only way for the cosine transform to decay at large  $|\eta|$  is to set

$$A = -\frac{\pi^2}{4}. \quad (7.12)$$

Making use of the transform

$$e^{-|\eta|} = \frac{2}{\pi} \int_0^\infty \frac{\cos \eta s}{1 + s^2} \, ds, \quad (7.13)$$

we then obtain  $C = \pi/2(1 + s^2)$ . Note that  $\int_0^\infty C(s) \, ds = \pi^2/4$ , whereby inspection of (7.7) and (7.9) reveals that the far-field condition (7.6) is satisfied. All that remains to impose is the inhomogeneous condition (7.3b), which simply gives  $f(\pi, s) = 0$ , that is,  $C \cosh \pi s + D \sinh \pi s = 0$ . Substitution into (7.10) then furnishes the kernel

$$f = \frac{\pi [\sinh s(\pi - \xi) \cos \xi + s \cosh s(\pi - \xi) \sin \xi]}{2(1 + s^2) \sinh \pi s}. \quad (7.14)$$

Since  $f$  is an even function of  $s$ , the integral appearing in Eq. (7.7) may be extended to the entire  $s$  axis; in the latter integral,  $\cos \eta s$  may be replaced by  $e^{i\eta s}$  [15]. Due to the even dependence upon  $\eta$  we may assume with no loss of generality that  $\eta > 0$ ; the resulting integral may be evaluated using contour integration. Thus, the integrand in Eq. (7.7) is integrated over a closed contour in the complex  $s$  plane consisting of the real axis and a large-radius semicircle in the half-plane  $\text{Im } s > 0$ , on which the magnitude of  $e^{i\eta s}$  is arbitrarily small. With  $f$  having simple poles at  $s = in$  ( $n = 1, 2, 3, \dots$ ), we find using the residue theorem

$$\int_0^\infty f(\xi, s) \cos \eta s ds = \frac{\pi e^{-\eta}}{4} (\pi - \xi + \cos \xi \sin \xi) + \frac{\pi}{2} \sum_{n=2}^\infty \frac{(-)^n e^{-n\eta}}{n^2 - 1} [n \cos n(\pi - \xi) \sin \xi + \cos \xi \sin n(\pi - \xi)]. \quad (7.15)$$

The series in Eq. (7.15) may actually be summed in closed form. Substituting into (7.7) and making use of (7.9) with (7.12) eventually gives the (real-valued) expression

$$\Psi = \frac{\pi}{4(\cos \xi - \cosh \eta)} \{(\xi - \pi) \cosh \eta + \sin \xi + \pi \cos \xi + [\pi - \xi + i \log(1 - e^{-\eta - i\xi}) - i \log(1 - e^{-\eta + i\xi})] \sinh \eta\}. \quad (7.16)$$

Although (7.16) was derived under the assumption  $\eta > 0$ , it is readily extended to  $\eta < 0$  based on the fact that  $\Psi$  is even in  $\eta$ .

We note that at large distances, where  $\xi, \eta \rightarrow 0$ , (7.16) gives

$$\Psi \sim -\frac{\pi}{2(\eta^2 + \xi^2)} \{2\xi + \eta[\pi - \arg(\eta + i\xi) + \arg(\eta - i\xi)]\}. \quad (7.17)$$

In the Appendix we analyze the behavior of  $\Psi$  close to the detachment points, showing that it reduces there to the local corner solution found by Mahadevan and Pomeau [1].

### VIII. DETERMINATION OF $\Omega$

Substituting (5.1) into the energy balance (4.7) yields, at leading order,

$$\iint \tilde{\mathbf{e}} : \tilde{\mathbf{e}} dx dy = \frac{\pi \Omega}{2}. \quad (8.1)$$

With its left-hand side being proportional to  $\Omega^2$ , (8.1) provides the condition for determining  $\Omega$ . With our velocity scaling being predicated upon the estimate of the contribution to the dissipation from the flat-spot region, it is tempting to infer that the left-hand side of (8.1) is provided by that contribution, say,

$$\iint \mathbf{E} : \mathbf{E} dX dY, \quad (8.2)$$

wherein  $\mathbf{E}$  is the symmetric part of the gradient of  $\mathbf{U}$  in the rescaled coordinates  $(X, Y)$  and the integration is carried out over the upper  $XY$  plane. However, the far-field approximation (7.17) implies that the latter integral diverges logarithmically. Indeed, making use of (5.3) and (7.2) we find that (7.17) reads

$$\Psi \sim -\frac{R}{2} \{2 \sin \theta + (\pi - 2\theta) \cos \theta\} \quad \text{for } R \gg 1, \quad (8.3)$$

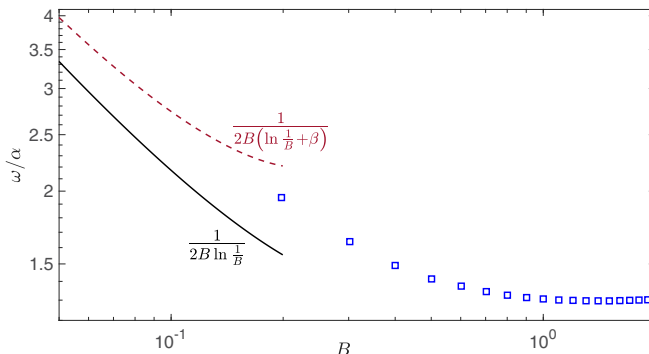


FIG. 3. Comparison with the numerical results of Wang [9], shown by the squares. The solid line depicts the logarithmically accurate leading-order approximation,  $\Omega \sim -(2 \ln B)^{-1}$ ; the dashed line portrays the algebraically accurate approximation (8.7) in which  $\beta$  is set to  $-0.4775$ .

with the resulting dissipation rate  $\mathbf{E} : \mathbf{E}$  being proportional to  $R^{-2}$ :

$$\mathbf{E} : \mathbf{E} \sim \frac{2\Omega^2}{R^2} \sin^2 \theta \quad \text{for } R \gg 1. \quad (8.4)$$

The above logarithmic divergence is the signature of the “intermediate” case in the asymptotic evaluation of integrals, where the dominant contribution is neither “local” nor “global” [12]. Indeed, anticipating that the leading-order correction to the rigid-body motion (5.2) is  $O(1)$  (see Sec. IX) and recalling that rigid-body motion does not contribute to the rate-of-strain tensor, we find that  $\tilde{\mathbf{e}} = O(1)$  in the drop-scale region. There is then no *a priori* reason to neglect the contribution from that region relative to the left-hand side of (8.1).

With that identification, we may readily evaluate the dissipation at a logarithmic leading order. We employ the “splitting” technique [12], introducing the parameter  $\lambda$ , which we choose to satisfy  $B \ll \lambda \ll 1$ . In terms of that parameter, the left-hand side of (8.1) becomes

$$\left( \iint_{r < \lambda} + \iint_{r > \lambda} \right) \tilde{\mathbf{e}} : \tilde{\mathbf{e}} \, dx \, dy. \quad (8.5)$$

The first integral in Eq. (8.5) is dominated by the flat-spot region, namely,

$$\iint_{R < \lambda/B} \mathbf{E} : \mathbf{E} \, dX \, dY, \quad (8.6)$$

which, upon substitution of (8.4), gives  $\pi \Omega^2 [\ln(\lambda/B) + O(1)]$ . Since (8.5) cannot depend upon the arbitrary parameter  $\lambda$ , the second integral there must cancel out the  $\ln \lambda$  term of the flat-spot contribution. As that integral is contributed at leading order by the drop-scale region, the second integral in Eq. (8.5) must be of the form  $\pi \Omega^2 [-\ln \lambda + O(1)]$ . [It cannot depend upon  $B$ , which does not appear in the  $O(1)$  problem of the drop-scale region.] Adding both contributions we obtain  $\pi \Omega^2 [\ln(1/B) + \beta]$  wherein the constant  $\beta$  is independent of  $B$ . Substitution into (8.1) furnishes the requisite approximation

$$\Omega \sim \frac{1}{2(\ln \frac{1}{B} + \beta)}. \quad (8.7)$$

The corresponding unscaled velocity is [cf. (2.3)]

$$\omega \sim \frac{\alpha}{2B(\ln \frac{1}{B} + \beta)}. \quad (8.8)$$

In Fig. 3 we compare approximation (8.8) with the numerical computations of Wang [9], as provided by Fig. 3.19 there. In these computations  $\alpha$  was set to  $10^\circ$ . A reasonable agreement is obtained for  $\beta = -0.4775$ . Note that the smallest Bond number for which Wang [9] provides data is 0.2.

## IX. DISCUSSION

Both the scaling analyses of Mahadevan and Pomeau [1] and that of Hodges *et al.* [8] are predicated upon the assumption that viscous dissipation is dominated by the flat-spot region. In contrast, our analysis shows that for two-dimensional drops dissipation in the flat-spot region is commensurate with that on the drop scale; the leading-order contribution in fact arises from the overlap between these two regions. As a consequence, the scaling of the drop speed with  $B$  differs from that suggested by Hodges *et al.* [8] by a logarithmic factor.

By exploiting the asymptotic overlap between the flat-spot and drop-scale regions, we have been able to extract the leading-order dissipation, and hence drop speed, from a local solution to the flow field in the flat-spot region. Since this leading-order approximation incurs a relative logarithmic error, it is quite crude. Our analysis, however, also provides a superior, algebraically accurate, approximation for the drop speed, in terms of a single constant  $\beta$  [cf. (8.8)], a pure number that is independent of  $B$ . We have not calculated  $\beta$ , though we have estimated its value based on extrapolation of numerical data. We note that to rigorously obtain  $\beta$  one would need to consider the deviation of the linearized drop-scale flow at  $O(1)$  from the leading  $O(B^{-1})$  rigid-body rotation. This deviation is driven by two mechanisms. The first arises from the need to match the  $O(1)$  flat-spot flow, which does not attenuate [cf. (8.3)]. The second is more subtle and has to do with the interaction between the  $O(B^{-1})$  rigid-body rotation [cf. (5.2)] and the  $O(B)$  deviations of the equilibrium drop boundary from a circle.

Our approximation scheme is based upon the smallness of both  $B$  and  $\alpha$ . In particular, the smallness of  $\alpha$  has facilitated our linearization scheme, where the leading-order drop shape is presumably unaffected by the flow. This assumption is tantamount to neglecting dynamic stresses as compared with the capillary pressure. In the flat-spot region, where the dimensionless velocity and length scale are  $O(1)$  and  $O(B)$ , respectively, the dimensional dynamic stress is of order  $\alpha\gamma/Ba$  (modulus the logarithmic dependence upon  $B$ ). Since the capillary pressure is of order  $\gamma/a$ , we find from the above *a posteriori* scrutinization that our scheme is valid provided  $\alpha \ll B$ . It may appear that the same condition is simply provided from the analysis of the drop-scale region, where the dimensionless velocity and length scale are  $O(1/B)$  and  $O(1)$ , respectively, while the capillary pressure scaling remains the same. In that region, however, the leading-order rigid-body motion does not result in dynamic stresses, and the estimate  $\alpha\gamma/Ba$  is nonrepresentative.

We conclude by revisiting the scaling analysis for three-dimensional drops, in light of the anomalous scaling predicted herein for two-dimensional drops. In the present dimensionless notation, the size of the flat-spot region is  $O(B^{1/2})$  [1,8]. Since velocity gradients associated with the leading rigid-body rotation are  $O(\omega)$ , the leading-order nonuniform flow in the flat-spot region is  $O(B^{1/2}\omega)$  and the contribution of the flat-spot region to viscous dissipation is  $O(\omega^2 B^{3/2})$ ; comparing the latter estimate to the  $O(B\alpha\omega)$  power of gravity yields the celebrated Mahadevan-Pomeau scaling,  $\omega = O(\alpha/B^{1/2})$ . Does the drop-scale flow contribute under that scaling? As in the two-dimensional problem, the deviation of the drop boundary from its reference shape (here a sphere) is still  $O(B)$ ; the interaction of the  $O(\alpha/B^{1/2})$  rigid-body motion with these deviations gives rise to  $O(\alpha B^{1/2})$  corrections to the rigid-body motion. Since the rate-of-strain tensor of a rigid-body motion trivially vanishes, it is evident that the drop-scale contribution to dissipation is  $O(\alpha^2 B)$ —subdominant to the  $O(\alpha^2 B^{1/2})$  local contribution. Assuming that the excess flow in the flat-spot region (relative

to the rigid-body motion) decays sufficiently fast, there is then no mechanism by which the drop-scale flow may enter the dominant dissipation balance. We accordingly expect that a local flow solution in the flat-spot region, comparable to the two-dimensional one derived in the present paper, would suffice to obtain a leading-order algebraically accurate approximation consistent with the Mahadevan-Pomeau scaling law.

#### ACKNOWLEDGMENTS

E.Y. was supported by the Israel Science Science Foundation (Grant No. 1081/16). We thank Michael Siegel for discussing with us the Ph.D. thesis of Xinli Wang. We are grateful to John Rallison for clarifying a technical point in Ref. [8].

#### APPENDIX: BEHAVIOR NEAR THE DETACHMENT POINTS

Consider the flow about the detachment point  $(\pi/2, 0)$ , corresponding to the limit  $\eta \gg 1$ . In that limit (7.16) gives

$$\Psi = -\frac{\pi^2 \cos \xi}{2} e^{-\eta} + \frac{\pi^2}{2} \left( 1 - 2 \cos^2 \xi - \frac{\xi}{\pi} + \frac{\sin 2\xi}{2\pi} \right) e^{-2\eta} + O(e^{-3\eta}). \quad (\text{A1})$$

Now, near that point we obtain from (7.1)

$$X - \pi/2 = \pi e^{-\eta} \cos \xi + \pi e^{-2\eta} \cos 2\xi + O(e^{-3\eta}), \quad (\text{A2a})$$

$$Y = \pi e^{-\eta} \sin \xi + O(e^{-2\eta}). \quad (\text{A2b})$$

In what follows, it is convenient to employ polar coordinates about the detachment point [cf. (5.3)],

$$X - \pi/2 = \varpi \cos \vartheta, \quad Y = \varpi \sin \vartheta. \quad (\text{A3})$$

In terms of these coordinates, (A2) give

$$\varpi = \pi e^{-\eta} + O(e^{-2\eta}), \quad \vartheta = \xi + O(e^{-\eta}). \quad (\text{A4})$$

Consider now the laboratory-frame streamfunction (6.7),

$$\Gamma = \frac{\varpi^2}{2} + \frac{\pi}{2} \left( X - \frac{\pi}{2} \right) + \Psi. \quad (\text{A5})$$

It is readily seen that the second term in Eq. (A5) cancels out with the leading  $O(e^{-\eta})$  term of (A1). [This is the reason for incorporating two successive terms in both (A1) and (A2a).] It follows that  $\Gamma = O(\varpi^2)$  near the detachment point, namely,

$$\Gamma = \frac{\varpi^2}{2} \left( 1 + \frac{\sin 2\vartheta}{2\pi} - \frac{\vartheta}{\pi} \right) + O(\varpi^3), \quad (\text{A6})$$

in agreement with Eq. (15) of Mahadevan and Pomeau [1].

- 
- [1] L. Mahadevan and Y. Pomeau, Rolling droplets, *Phys. Fluids* **11**, 2449 (1999).
  - [2] D. Quéré, Non-sticking drops, *Rep. Prog. Phys.* **68**, 2495 (2005).
  - [3] D. Richard and D. Quere, Viscous drops rolling on a tilted non-wettable solid, *Europhys. Lett.* **48**, 286 (1999).
  - [4] P. Aussillous and D. Quere, Liquid marbles, *Nature (London)* **411**, 924 (2001).
  - [5] M. R. Rahman and P. R. Waghmare, Influence of outer medium viscosity on the motion of rolling droplets down an incline, *Phys. Rev. Fluids* **3**, 023601 (2018).

- [6] C. Huh and L. E. Scriven, Hydrodynamic model of steady movement of a solid/liquid/fluid contact line, *J. Colloid Interface Sci.* **35**, 85 (1971).
- [7] D. J. Benney and W. J. Timson, The rolling motion of a viscous fluid on and off a rigid surface, *Stud. Appl. Math.* **63**, 93 (1980).
- [8] S. R. Hodges, O. E. Jensen, and J. M. Rallison, Sliding, slipping and rolling: The sedimentation of a viscous drop down a gently inclined plane, *J. Fluid Mech.* **512**, 95 (2004).
- [9] X. Wang, On the rolling motion of viscous fluid on a rigid surface, Ph.D. thesis, New Jersey Institute of Technology (2008).
- [10] B. M. Mognetti, H. Kusumaatmaja, and J. M. Yeomans, Drop dynamics on hydrophobic and superhydrophobic surfaces, *Faraday Discuss.* **146**, 153 (2010).
- [11] S. P. Thampi, R. Adhikari, and R. Govindarajan, Do liquid drops roll or slide on inclined surfaces? *Langmuir* **29**, 3339 (2013).
- [12] E. J. Hinch, *Perturbation Methods* (Cambridge University Press, Cambridge, 1991).
- [13] S. W. Rienstra, The shape of a sessile drop for small and large surface tension, *J. Eng. Math.* **24**, 193 (1990).
- [14] J. Happel and H. Brenner, *Low Reynolds Number Hydrodynamics* (Prentice-Hall, Englewood Cliffs, NJ, 1965).
- [15] A. M. J. Davis and M. E. O'Neill, Separation in a Stokes flow past a plane with a cylindrical ridge or trough, *Q. J. Mech. Appl. Math.* **30**, 355 (1977).
- [16] D. J. Jeffrey, The temperature field or electric potential around two almost touching spheres, *J. Inst. Math. Appl.* **22**, 337 (1978).